Journal of Catalysis 268 (2009) 26–38

Contents lists available at ScienceDirect

Journal of Catalysis

journal homepage: www.elsevier.com/locate/jcat

Remarkably fast oxidation of alkanes by hydrogen peroxide catalyzed by a tetracopper(II) triethanolaminate complex: Promoting effects of acid co-catalysts and water, kinetic and mechanistic features

Marina V. Kirillova [a], Yuriy N. Kozlov [b], Lidia S. Shul'pina [c], Oleg Y. Lyakin [d], Alexander M. Kirillov [a], Evgenii P. Talsi [d], Armando J.L. Pombeiro [a,*], Georgiy B. Shul'pin [b,*]

[a] Centro de Química Estrutural, Complexo I, Instituto Superior Técnico, TU Lisbon, Av. Rovisco Pais, 1049-001 Lisbon, Portugal
[b] Semenov Institute of Chemical Physics, Russian Academy of Sciences, Ulitsa Kosygina, dom 4, Moscow 119991, Russia
[c] Nesmeyanov Institute of Organoelement Compounds, Russian Academy of Sciences, Ulitsa Vavilova, dom 28, Moscow 119991, Russia
[d] Boreskov Institute of Catalysis, Russian Academy of Sciences, Prospekt Akad. Lavrentieva, dom 5, Novosibirsk 630090, Russia

ARTICLE INFO

Article history:
Received 15 June 2009
Revised 25 August 2009
Accepted 29 August 2009
Available online 29 September 2009

Keywords:
Alkanes oxidation
Acid promoters
Copper complexes
Cyclohexane
Homogeneous catalysis
Hydrogen peroxide
Water

ABSTRACT

The kinetic and mechanistic features of alkane oxidations to the corresponding alkyl hydroperoxides (main primary products), alcohols and ketones (secondary products) in the systems composed of tetracopper(II) triethanolaminate catalyst $[O\subset Cu_4\{N(CH_2CH_2O)_3\}_4(BOH)_4][BF_4]_2$ (**1**), aqueous hydrogen peroxide, acetonitrile solvent and an acid promoter (co-catalyst), have been investigated based on the combination of experimental kinetic, selectivity, ESR and UV–vis methods. The nature of acid promoter (hydrochloric, sulfuric, nitric and trifluoroacetic acid) is shown to be a key factor affecting significantly the rate of alkane oxidation. Although all these acids exhibit noticeable promoting effect, it has been observed that in the presence of HCl the reaction proceeds extremely rapidly, being one order faster than those promoted by the other acids, and allowing to achieve the remarkably high turnover frequencies (TOFs) of ca. 600 h^{-1}. The unusual rate-accelerating role of water has also been disclosed in the oxidation of cyclohexane catalyzed by **1** + HCl or **1** + CF_3COOH systems. Furthermore, uncommon second-order reaction kinetics with respect to the catalyst have been found. A mechanism of the alkane oxygenation has been proposed, which includes the formation of hydroxyl radicals attacking the alkane molecule. Hydroxyl radicals are formed via the interaction between H_2O_2 and catalytically active Cu(I) species, the latter being reversibly generated from **1** under the action of an acid, H_2O_2 and water.

1. Introduction

The development of new atom and energy efficient routes for the selective and green oxidative transformation of saturated hydrocarbons (main components of oil, natural gas and seabed) to yield industrially valuable products constitutes a challenge to various areas of modern chemistry and, in particular, to catalysis [1–8]. Due to the high inertness of alkanes, their oxidation reactions typically undergo in the presence of metal catalysts [1–4], require elevated temperatures and pressures, and/or the presence of strongly acidic reaction media [9–11]. An alternative approach consists of the development of new bioinspired catalysts that are capable to transform alkanes efficiently and selectively under relatively mild reaction conditions.

In particular, compounds of copper (an environmentally relatively acceptable and cheap metal) are known to catalyze oxygenations [1–4,12,13] of hydrocarbons [7–36] with peroxides or molecular oxygen [37–46] as oxidants. The high activity of Cu compounds can be associated with the effectiveness of copper in particulate methane monooxygenase (pMMO), an enzyme that bears a multicopper cluster with N,O-environment and can catalyze the hydroxylation of alkanes [47,48]. Recently, some of us have reported a series of self-assembled multicopper(II) compounds with N,O-ligands [30–36,49–51], and applied them as catalysts for (i) the mild oxidation of alkanes to alcohols and ketones [30–36], (ii) the aqueous-medium carboxylation of alkanes to carboxylic acids [52] and (iii) the aerobic oxidation of benzylic alcohols to aldehydes [53]. It has been found that the tetracopper(II) triethanolaminate complex $[O\subset Cu_4\{N(CH_2CH_2O)_3\}_4(BOH)_4][BF_4]_2$ (**1**) (Scheme 1) is one of the most active copper catalysts for the mild oxidation of cyclohexane [30,31], its activity being drastically accelerated by the presence of nitric acid additive (co-catalyst), leading to 39% yields (based on C_6H_{12}) of oxygenated products in a single batch.

---

* Corresponding authors. Fax: +351 21 8464455 (A.J.L. Pombeiro); +7 495 9397417/6512191 (G.B. Shul'pin).
E-mail addresses: pombeiro@ist.utl.pt (A.J.L. Pombeiro), Shulpin@chph.ras.ru, gbsh@mail.ru (G.B. Shul'pin).

0021-9517/$ - see front matter © 2009 Elsevier Inc. All rights reserved.
doi:10.1016/j.jcat.2009.08.016

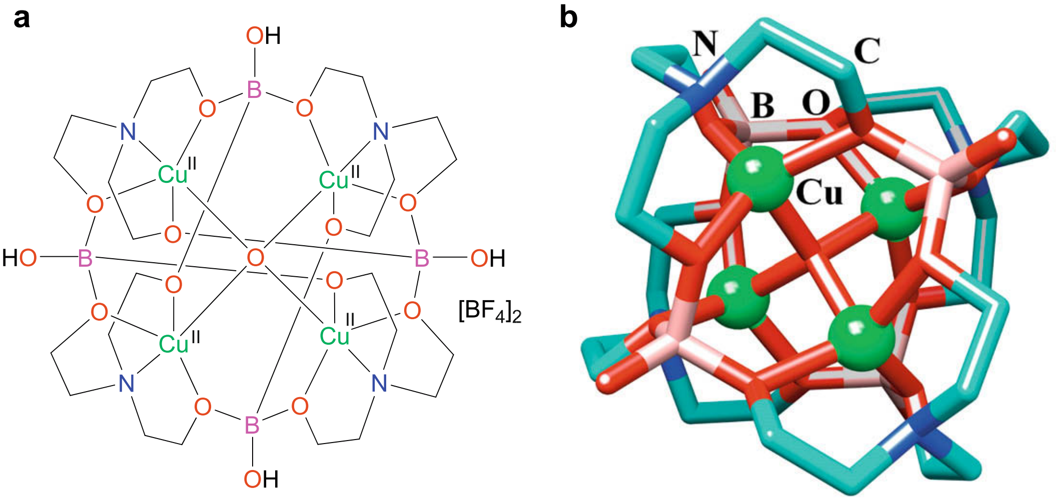

Scheme 1. Structural formula (a) and X-ray crystal structure (b) of compound **1** [30]. On drawing (b) counter ions and H atoms are omitted for clarity. Colour codes: Cu green, O red, N blue, C cyan, B pink. (For interpretation of the references to colour in this figure legend, the reader is referred to the web version of this article.)

In spite of the progresses achieved in the mild oxidation of alkanes with **1** and hydrogen peroxide as an oxidant [30,31], the promoting effects of other acids, reaction kinetics and mechanism remained unstudied, and thus constitute a main objective of the current work. Apart from its high activity, the choice of **1** as a catalyst in the present study is governed by its hydrosolubility, possibility of recycling, as well as its facile aqueous-medium self-assembly synthesis from rather cheap and readily available chemicals [30,31]. Besides, compound **1** possesses a high stability that is associated with its intricate cage-like structure, where four copper(II) atoms are clustered through the triethanolaminate μ_3-O atoms and μ_3-B-OH groups, being further stabilized by the "central" μ_4-O oxo atom [30].

It should be noted that the primary scope of the present work consists of shedding some light on the kinetics and mechanism of alkane oxidations with **1**, and of establishing the role of different acid promoters and water in those reactions, whereas their detailed optimization in terms of efficiency and rational consumption of reagents lies beyond the scope of this study. In fact, it has also been found herein that under certain reaction conditions a substantial consumption of hydrogen peroxide oxidant in side reactions (e.g. catalase activity) is occurring, being dependent on the type of acid promoter and the relative concentrations of all reaction components.

Hence, based on a combination of experimental kinetic and selectivity studies, ESR and UV–vis spectroscopic methods, we report herein the kinetic and mechanistic features of mild alkane oxidations in the systems composed of **1**, aqueous hydrogen peroxide, acetonitrile and an acid additive (the latter being selected from hydrochloric, trifluoroacetic, nitric, sulfuric and acetic acids), and show how the reaction rates are dramatically affected by the type of used acid co-catalyst. These features include (i) the remarkably fast oxidation of cyclohexane in the presence of hydrochloric acid additive (TOFs up to ca. 600 h^{-1}), (ii) the unusual rate-accelerating role of water and (iii) the uncommon second-order (with respect to catalyst) reaction kinetics in cyclohexane oxidation.

2. Experimental

2.1. Materials and methods

All chemicals were obtained from commercial sources and were used as received. Catalyst **1** has been prepared according to the previously described procedure [30].

The ESR spectra (−196 °C) were recorded on a Bruker ER-200D spectrometer at 9.3–9.4 GHz, modulation frequency of 100 kHz, modulation amplitude of 5 G. The dual ESR cavity furnished with the spectrometer was used. Periclase crystal (MgO) with impurities of Mn^{2+} and Cr^{3+}, which served as a side reference, was placed into the second compartment of the dual cavity. Measurements were conducted in a quartz finger Dewar filled with liquid nitrogen. Samples were prepared in quartz ESR tubes (d = 3 mm). For kinetic ESR studies, the sample was placed in a thermostat at the required temperature directly in the ESR tube. To stop the reaction, the tube was immersed in liquid nitrogen, followed by registration of the ESR spectrum at −196 °C. After the spectrum registration was complete, the sample was again placed in the thermostat. ESR signals were quantified by double integration with a frozen solution of copper(II) acetylacetonate as a standard at −196 °C. The relative accuracy of the quantitative ESR measurements was ±30%.

The UV–vis spectra were recorded (2 min after the components were mixed) on a Jasco model 7800 UV–vis spectrophotometer at ambient (ca. 25 °C) temperature.

2.2. Alkane oxidations

The reactions of alkanes were typically carried out in air in thermostated Pyrex cylindrical vessels with vigorous stirring and using MeCN as a solvent (**CAUTION**: the combination of air or molecular oxygen and H_2O_2 with organic compounds at elevated temperatures may be explosive!). Typically, catalyst **1** and the co-catalyst (an acid) were introduced into the reaction mixture in the form of stock solutions in water and acetonitrile, respectively. The substrate was then introduced and the reaction started when hydrogen peroxide (50% in H_2O) was added in one portion. The reactions were stopped by cooling and were analyzed by GC using a Fisons Instruments GC 8000 series gas chromatograph with a capillary column 30 m × 0.32 mm × 25 μm, DB-WAX (J&W) (helium was the carrier gas; nitromethane was the internal standard). Since the oxygenation of alkanes usually gives rise to the formation of the corresponding alkyl hydroperoxides as the main primary products, their quantification was performed by a simple method developed earlier by some of us [54–56]. In our kinetic studies for precise determination of oxygenate concentrations only data obtained after reduction of the reaction sample with PPh_3 were usually used, taking into account that the original reaction mixture typically contained the three products, cyclohexyl hydroperoxide (as a primary product), cyclohexanone and cyclohexanol.

3. Results

In the present work, we have used cyclohexane as a recognized substrate model [57], also in view of the importance of the products (i.e. cyclohexanol and cyclohexanone are intermediates in nylon-6,6′ and polyamide-6 productions) [57,58], whereas other alkanes (Table 1) have been applied in the selectivity tests. Hence, heating a solution of cyclohexane, CyH, in acetonitrile at 50 °C with 50% aqueous hydrogen peroxide in the presence of compound **1** leads to a slow oxygenation of the alkane (Fig 1, curve 1a). As expected [30–34,36], the reaction is noticeably accelerated if an acid promoter (ca. 10 equivalents relatively to catalyst) is added. Examples of the kinetic curves of the reactions co-catalyzed by nitric, acetic, trifluoroacetic (TFA), sulfuric and hydrochloric acids under various conditions are shown in Figs. 1 and 2. The oxidation in the presence of sulfuric acid occurs with an auto-acceleration and gives finally cyclohexanone as the main product (after PPh_3) (Fig. 2, graph c). Although all tested acids exhibit noticeable promoting effects, we have unexpectedly observed that in the presence of HCl the reaction proceeds extremely rapidly (Fig. 2, graph d), being one order faster than those promoted by the other acids, although under the used conditions the reagents conversion into the oxygenated products does not increase to values beyond 5–6%. Taking also into consideration that the oxidations occur rather efficiently in the presence of TFA, the current study focused on the detailed investigation of the promoting effects of HCl and TFA.

3.1. Oxidation in the presence of HCl

The oxidation of cyclohexane in the presence of HCl is very fast and can be completed in ca. 10 min under, e.g. the reaction conditions shown in Fig. 2d. At this time, the reaction mixture contains (after reduction with PPh_3) cyclohexanol and cyclohexanone in approximately equal concentrations (Fig. 2, graph d). This testifies [54–56] that cyclohexyl hydroperoxide formed as the primary product is rapidly decomposed in the course of the reaction to more stable cyclohexanone and cyclohexanol. Indeed, when cyclohexyl hydroperoxide is present in the reaction solution in relatively high concentration (for examples, see below) the reduction of the samples with PPh_3 gives predominantly cyclohexanol.

The oxidation process is accompanied with changes in the electronic spectra of the solution (Fig. 3). Addition of HCl to the solution of **1** and cyclohexane leads to some decrease of the absorptions with maxima at ca. 750 and 950 nm. When H_2O_2 is added, the intensities of the both bands become lower. Among all the components of the reaction solution, only copper complexes absorb light in the λ region above 400 nm. Hence, the registered changes in the electronic spectra indicate that the starting complex is changing in the course of the alkane oxidation reaction, by generating the active species with the formation of Cu(I) intermediates (see below). Acetonitrile and chloride ions as a ligands can stabilize copper(I) complexes towards the oxidation, and we can assume that the rate constant of the Cu(II) regeneration via the oxidation of Cu(I) by H_2O_2 is not high. As a result, the amount of low-valent copper in the course of the catalytic process can be relatively high. This conclusion is supported additionally by the ESR method (see below). The presence at ca. 720 nm of an isosbestic point (as confirmed later) at the initial period of the oxidation indicates that the starting tetramer **1** is transformed in the beginning of the reaction into only one light-absorbing species. It should be noted that an unidentified absorbance minimum has also been observed in all spectra at ca. 945 nm.

The ESR spectra of the reaction solution in the course of the interaction of **1** with HCl exhibit an anisotropic signal at about $g = 2.13$ with peak-to-peak width of 200 G (Fig. 4), being diagnostic of low-spin $S = 1/2$ copper(II) complexes, either mononuclear or multinuclear ones with at least one non-interacting copper atom. The ESR signal shape in Fig. 4 becomes more symmetric with time indicating some minor changes in the generated copper(II) complex structure in the course of the interaction with HCl. The total concentration of the generated copper(II) species grows during the initial period and becomes approximately stable after 20 min of the reaction (Fig. 5).

We studied the dependence of the initial rate W_0 of cyclohexane oxidation on the concentration of catalyst **1** (Fig. 6). As compound **1** was introduced into the reaction mixture in the form of a stock solution in H_2O, the water concentration increased on rising the

Table 1
Selectivity parameters in the oxidation of alkanes.[a]

Entry	System	C(1):C(2):C(3):C(4)		1°:2°:3°	*trans*/*cis*	
		n-Heptane	*n*-Octane	Methylcyclohexane	*cis*-DMCH	*trans*-DMCH
1	**1**–HCl–H_2O_2 (MeCN, 50 °C)		1.0:4.3:3.7:3.4	1:13:22	0.9	1.0
2	**1**–CF_3COOH–H_2O_2 (MeCN, 50 °C)	1.0:8.4:6.7:5.3	1.0:5.1:5.2:4.3	1:5:14	0.8	0.8
3	**1**–HNO_3–H_2O_2 (MeCN, 50 °C)	1.0:6.5:6.5:5.5			0.84	0.85
4	$Cu(NO_3)_2$–HNO_3–H_2O_2 (MeCN, 50 °C)	1.0:6.7:6.0:4.7			0.85	0.74
5	VO_3^-–PCA–H_2O_2 (MeCN, 40 °C)[b]	1:9:7:7	1:7:7.5:5	1:6:18	0.75	0.8
6	VO_3^-–H_2SO_4–H_2O_2 (MeCN, 50 °C)[c]	1:7:6.5:6.5	1:10:10.5:8.5	1:7:26	0.85	0.90
7	hν–H_2O_2 (MeCN, 20 °C)	1:7:6:7			0.9	
8	$FeSO_4$–H_2O_2 (MeCN, 20 °C)	1:5:5:4.5			1.3	
9	$Ni(ClO_4)_4$ –H_2O_2 (MeCN, 70 °C)[d]	1:6.3:7.2:6.1		1:7:15		
10	**2**-H_2O_2 (MeCN, 60 °C)[e]	1:5.5:5.0:4.6		1:4:10	0.9	
11	$NaAuCl_4$–H_2O_2 (MeCN, 75 °C)[f]	1:35:25:23		1:116:255		
12	**3**–$MeCO_2H$–H_2O_2 (MeCN, 25 °C)[g]	1:46:35:34	1:29:25:24	1:26:200	0.34	4.1

[a] Reaction conditions for entries 1–3 are similar to those used in the experiments shown in Figs. 1 and 2. All parameters were measured after the reduction of the reaction mixtures with triphenylphosphine before GC analysis and calculated based on the ratios of isomeric alcohols. The calculated parameters from the concentrations of alcohols after reduction with PPh_3 were normalized, i.e., recalculated taking into account the number of hydrogen atoms at each carbon. Parameters C(1):C(2):C(3):C(4) are relative reactivities of hydrogen atoms at carbons 1, 2, 3 and 4 of the *n*-heptane or *n*-octane chain. Parameters 1°:2°:3° are relative normalized reactivities of the hydrogen atoms at primary, secondary and tertiary carbons of branched alkanes. Parameter *trans*/*cis* is determined as the ratio of the formed tertiary alcohol isomers with mutual *trans* and *cis* orientation of the methyl groups. Abbreviations: MCH is methylcyclohexane; *cis*-DMCH and *trans*-DMCH are isomers of 1,2-dimethylcyclohexane.

[b] PCA is pyrazine-2-carboxylic acid. For this system, see [61,62].

[c] For this system, see [72].

[d] In the presence of TMTACN (1,4,7-trimethyl-1,4,7-triazacyclononane). For this system, see [73].

[e] Compound **2** is the complex (2,3-η-1,4-diphenylbut-2-en-1,4-dione)undecacarbonyl triangulotriosmium. For this system, see [74].

[f] For this system, see Ref. [75].

[g] Compound **3** is the complex $[Mn_2L_2(\mu\text{-}O)_3]^{2+}$ where L is 1,4,7-trimethyl-1,4,7-triazacyclononane. For this system, see [64,76].

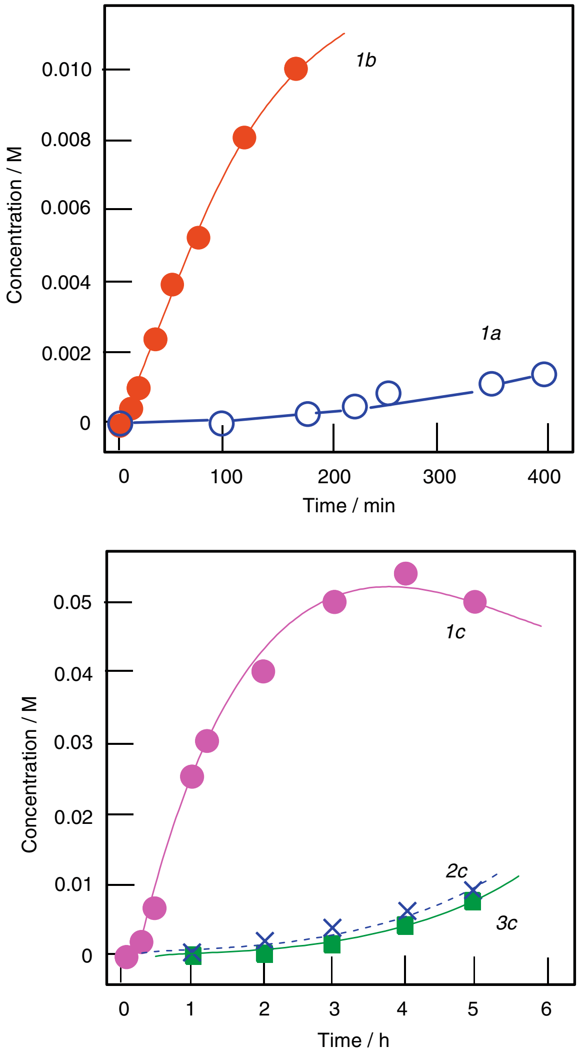

Fig. 1. Accumulation of cyclohexyl hydroperoxide (curves 1), cyclohexanol (curve 2) and cyclohexanone (curve 3) with time in the cyclohexane oxidation with hydrogen peroxide catalyzed by compound **1** (1 mM) under different conditions. Solvent was acetonitrile (total volume of the reaction solution was 5 mL); 50 °C. Other conditions. Curve a: cyclohexane, 0.46 M; H_2O_2, 0.5 M; no acid additive. Curve b: cyclohexane, 0.46 M; H_2O_2, 0.5 M; HNO_3, 10 mM. Curve c: cyclohexane, 0.74 M; H_2O_2, 1.2 M; HNO_3, 1 mM. Amounts of cyclohexanone and cyclohexanol were determined twice, before and after reduction of the aliquots with solid PPh_3 (for this method, see [54–56]).

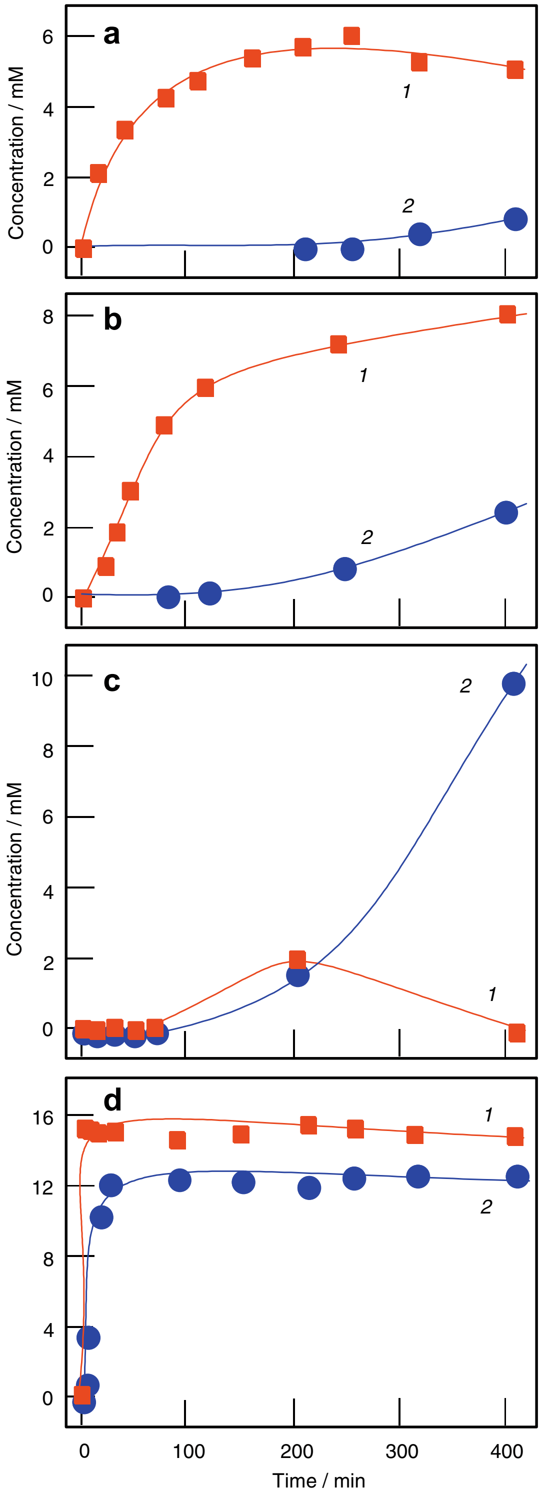

Fig. 2. Cyclohexane oxidation with hydrogen peroxide catalyzed by compound **1** (1 mM) in the presence of different acids (10 mM): CH_3COOH (a), CF_3COOH (b), H_2SO_4 (c) and HCl (d). The kinetic curves for the accumulation of cyclohexanol (curve 1) and cyclohexanone (curve 2) with time obtained after the reduction of the aliquots with solid PPh_3 are shown. Conditions: cyclohexane, 0.46 M; H_2O_2, 0.5 M; the total content of water in the reaction mixture was 2.16 M; 50 °C; solvent was acetonitrile (total volume of the reaction solution was 5 mL).

concentration of **1** (Fig. 6, curve 1). In a special set of experiments, H_2O was added to maintain the constant water concentration (1.61 M; Fig. 6, curve 2) in all reactions. It can be clearly seen that in both cases the dependence curves have an S-shape.

Two sets of experiments at different constant concentrations of water have been carried out to evaluate the dependence of initial oxidation rate on the concentration of HCl co-catalyst. In the first set, water concentration was 1.17 M being dependent on the concentration of added aqueous HCl (Fig. 7, curve 1). In the second set, the oxidations were carried out at a higher fixed concentration of water (4.0 M; Fig. 7, curve 2). As it can be seen from Fig. 7, in both cases the curves have maxima at the $[HCl]_0$ of 1.50 (curve 1) or 4.50 (curve 2). Such a difference in the maxima position apparently indicates that the initial reaction rate W_0 also depends on the concentration of water. This has been confirmed in a separate experiment (Fig. 8), which demonstrates that the increase of the total water concentration $[H_2O]_{total}$ in the reaction mixture from 1 to 4 M leads to a drastic acceleration of the reaction, resulting in the W_0 growth from ca. 15×10^{-6} to 110×10^{-6} M s^{-1}. However, further augmentation of the $[H_2O]_{total}$ above 4 M (optimal value) is not favourable giving a W_0 drop. To our knowledge, such a rate-accelerating role of water in the reaction of cyclohexane oxi-

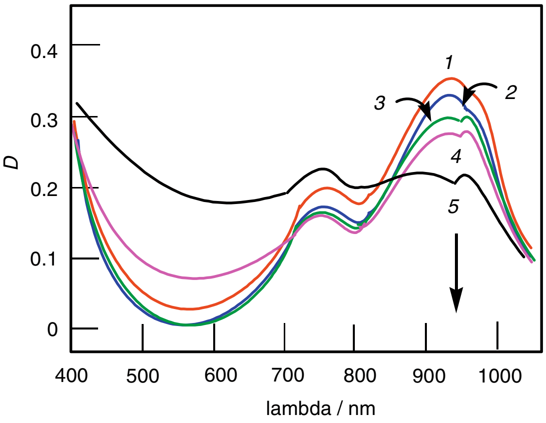

Fig. 3. Changes in the electronic spectrum of the solution in the course of the cyclohexane oxidation reaction. Conditions: 50 °C; solvent was acetonitrile (total volume of the reaction solution was 5 mL). Curves 1: a solution of **1** (1 mM) and cyclohexane (0.46 M); 2: HCl (4 mM) is added; 3: H_2O_2 (0.5 M) is added; 4: 10 min after the addition of H_2O_2; 5: 65 min after the addition of H_2O_2.

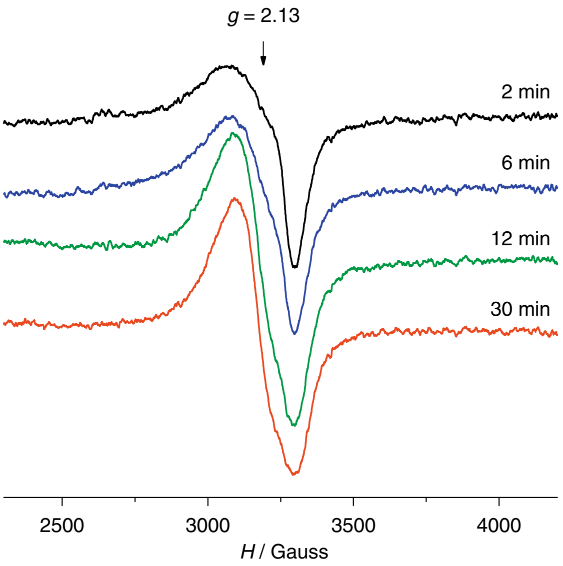

Fig. 4. Changes in the ESR spectra of the solution of **1** (1 mM) and HCl (4 mM) with time (for conditions, see Fig. 5).

dation is unusual and constitutes an important feature of the present system. Although a remarkable accelerating effect of H_2O as a co-solvent in the catalytic oxidation of catechols with a dinuclear Cu(II) complex has been reported recently [59], such a promoting role of water with respect to alkane transformations is limited to single studies [52,60].

The dependence of W_0 on the initial concentration of cyclohexane reaches a plateau at $[CyH]_0 > 0.2$ M (Fig. 9), while the dependence on the initial concentration of hydrogen peroxide is linear at $[H_2O_2]_0 < 0.6$ M (Fig. 10). The latter figure also features an example of remarkably fast oxidation of cyclohexane in the presence of HCl additive, which is characterized by a very high value of W_0 (ca. 135×10^{-6} M s^{-1}). This W_0 value is significantly higher than those typically obtained in the analogous reaction promoted by TFA (see below), or in the other alkane oxidation systems based on, e.g., vanadium [54–56,61,62], iron [63] and manganese [64] catalysts previously studied by some of us. Yet another feature of the present catalytic system (**1** + HCl) consists in the very high turnover frequencies (TOFs) (moles of oxidation products per mol of catalyst per hour) that reach values of up to ca. 600 h^{-1} (e.g. under the reaction conditions of Fig. S1a, graph e).

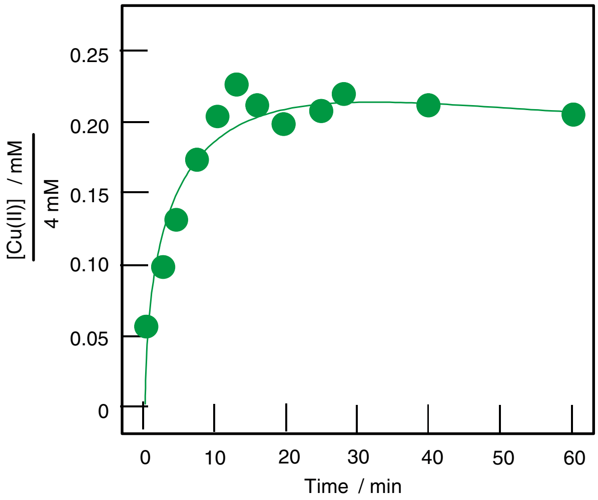

Fig. 5. Changes in the ESR spectrum of the solution of compound **1** (1 mM) in $MeCN/H_2O$ (10:1 v/v) mixture after the addition of HCl (4 mM). The reaction was carried out at 50 °C, the ESR spectra were recorded at liquid nitrogen temperature. The [Cu(II)] (mM)/4 mM ratio (dimensionless value, where 4 mM is the total initial concentration of the four Cu^{II} of **1**) versus time is plotted. For original ESR spectra, see Fig. 4.

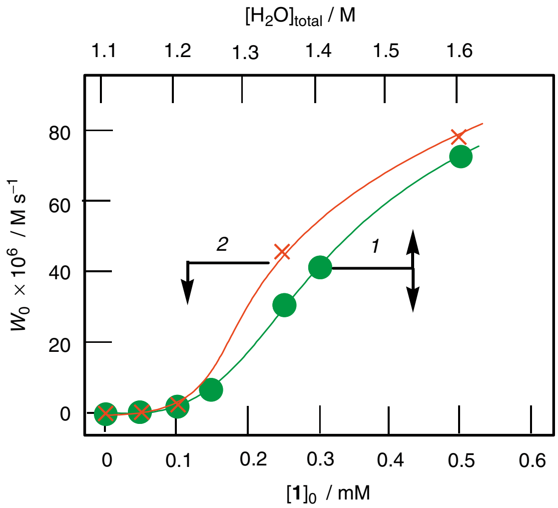

Fig. 6. Oxidation of cyclohexane (0.46 M) with hydrogen peroxide (50% aqueous; 0.5 M) catalyzed by compound **1** in the presence of HCl (4 mM) in MeCN at 50 °C. Dependences of the initial rate of oxygenate formation W_0 on initial concentration of **1** are shown. Curve 1: the oxidation at varied concentration of water in the interval 1.11–1.61 M; curve 2: the oxidation at constant in all experiments total concentration of water (1.61 M). Concentrations of cyclohexanone and cyclohexanol were determined after the reduction of the aliquots with solid PPh_3. For the original full kinetic curves, see Fig. S1.

3.2. Oxidation in the presence of CF_3COOH

The cyclohexane oxidation in the presence of trifluoroacetic acid typically proceeds one order slower than that promoted by HCl, and an auto-acceleration can be clearly seen (Fig. 11, curve 1). In further studies, as the processes occur with auto-acceleration, we measured the maximum rate W_0 from the slope of the dotted line (Fig. 11, curve 1a) of the reaction after the lag period. In a special experiment, all components, except H_2O_2, were mixed in the beginning of the reaction and the system was incubated for

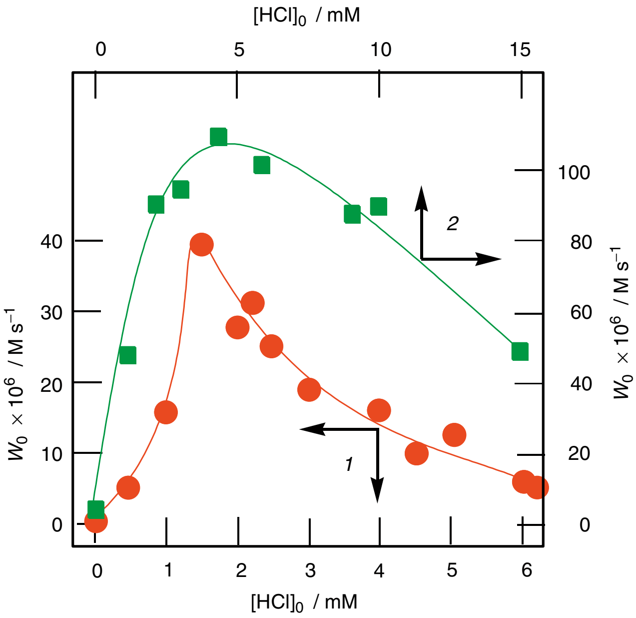

Fig. 7. Oxidation of cyclohexane (0.46 M) with hydrogen peroxide (50% aqueous; 0.5 M) at two different concentrations of water (curve 1: $[H_2O] = 1.17$ M; curve 2: $[H_2O] = 4.0$ M) catalyzed by compound **1** (0.1 mM) in the presence of HCl in MeCN at 50 °C. Dependences of the initial rate of oxygenate formation W_0 on concentration of added HCl are shown. Concentrations of cyclohexanone and cyclohexanol were determined after the reduction of the aliquots with solid PPh_3. For the original full kinetic curves, see Figs. S2 and S3.

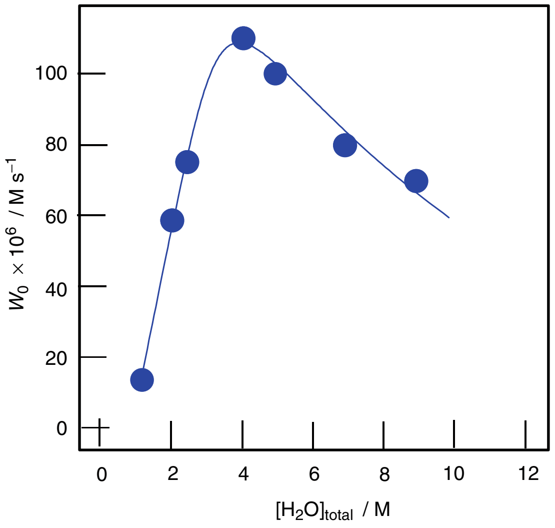

Fig. 8. Oxidation of cyclohexane (0.46 M) with hydrogen peroxide (50% aqueous; 0.5 M) catalyzed by compound **1** (0.1 mM) in the presence of HCl (4 mM) in MeCN at 50 °C. Dependence of the initial rate of oxygenate formation W_0 on total concentration of water present in the solution is shown. Concentrations of cyclohexanone and cyclohexanol were determined after the reduction of the aliquots with solid PPh_3. For the original full kinetic curves, see Fig. S4.

60 min prior to the addition of hydrogen peroxide (Fig. 11, curve 2). The kinetic curve for the accumulation of oxygenates in this case was very similar to curve 1. It can be, thus, concluded that heating of compound **1** and TFA does not lead to the formation of a catalytically active species. In the second special experiment, the reaction was incubated with **1**, TFA and H_2O_2 for 30 min prior the addition of cyclohexane. In this case, the oxidation proceeds much faster (Fig. 11, curve 3). Based on this experiment, we can conclude that a catalytically active species is formed in the interaction between **1**, TFA and H_2O_2. Curve 1 shows that the oxidation process stops after 60 min. However, if we add a new portion of hydrogen peroxide the reaction continues and this procedure can be repeated (Fig. 11, curve 4). This experiment testifies that the catalytic species is not deactivated in the course of the oxidation process, being in accord with the recognized ability of **1** to be multiply recycled [31].

The oxidation is accompanied with changes in the electronic spectra of the solution (Fig. 12). Addition of TFA to the mixture of **1** and CyH leads to some decrease of the absorptions with maxima at ca. 750 and 950 nm. When H_2O_2 is added, the intensities of both bands become lower. Similar changes can be noticed further when the oxidation occurs. All changes proceed with an isosbestic

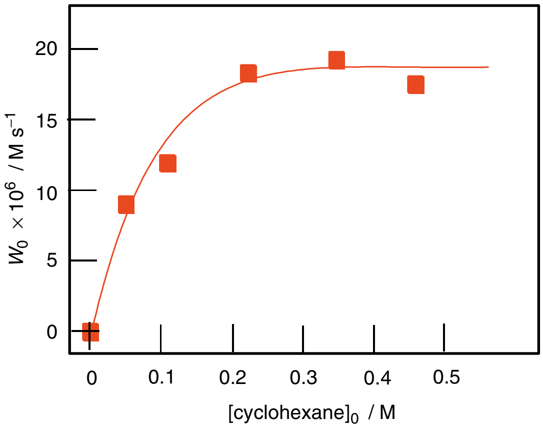

Fig. 9. Oxidation of cyclohexane with hydrogen peroxide (50% aqueous; 0.5 M; the total content of water in the reaction mixture was 1.17 M) catalyzed by compound **1** (0.1 mM) in the presence of HCl (4 mM) in MeCN at 50 °C. Dependence of the initial rate of oxygenate formation W_0 on initial concentration of cyclohexane is shown. Concentrations of cyclohexanone and cyclohexanol were determined after reduction of the aliquots with solid PPh_3. For the original full kinetic curves, see Fig. S5.

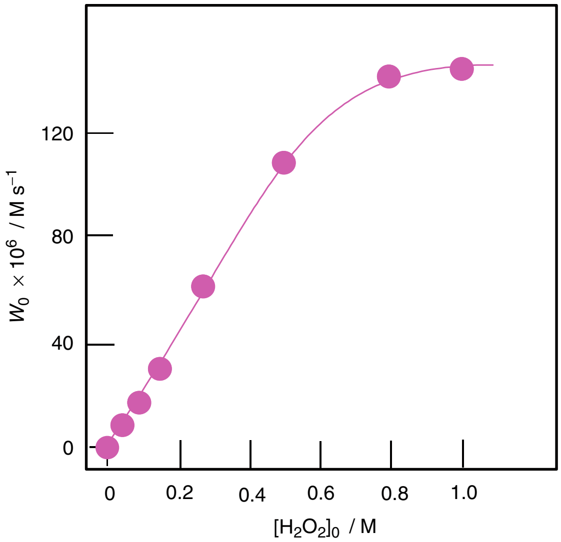

Fig. 10. Oxidation of cyclohexane with hydrogen peroxide (50% aqueous; the total content of water in the reaction mixture was constant = 4.0 M) catalyzed by compound **1** (4 mM) in the presence of HCl (4 mM) in MeCN at 50 °C. Dependence of the initial rate of oxygenate formation W_0 on initial concentration of H_2O_2 is shown. Concentrations of cyclohexanone and cyclohexanol were determined after reduction of the aliquots with solid PPh_3. For the original full kinetic curves, see Fig. S6.

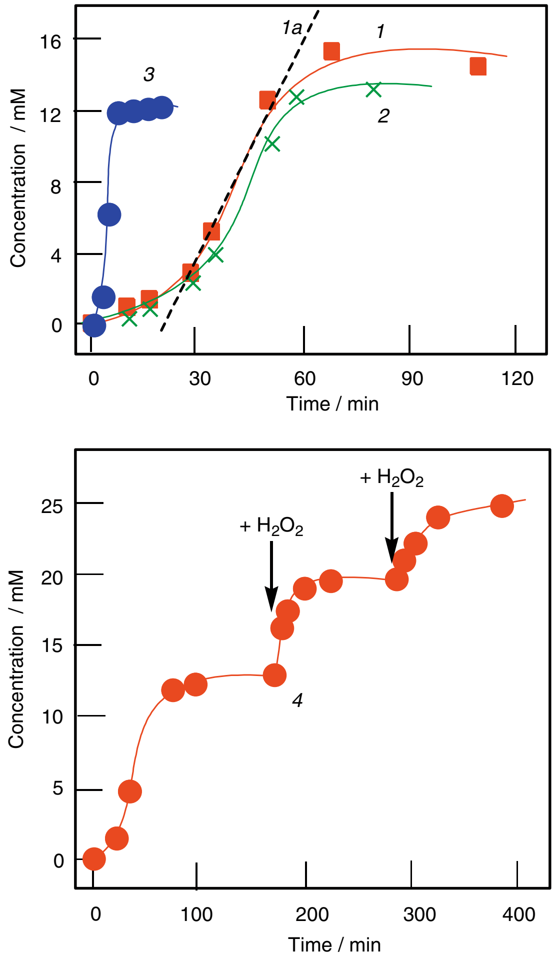

Fig. 11. Accumulation of oxygenates with time in the cyclohexane (0.46 M) oxidation with hydrogen peroxide (0.5 M) catalyzed by compound **1** (1 mM) in the presence of TFA (4 mM) and H_2O (3.27 M). Solvent was acetonitrile (total volume of the reaction solution was 5 mL); 50 °C. Curve 1: all components were mixed at time = 0. Curve 2: a solution of **1** and TFA was stirred during 60 min and then at time = 0 cyclohexane and H_2O_2 were added. Curve 3: a solution of **1**, TFA and H_2O_2 was stirred during 30 min and then at time = 0 cyclohexane was added. Curve 4: at moments denoted by arrows new portions of H_2O_2 (0.5 M) were added.

point at ca. 720 nm. The changes in the spectrum are similar to those observed in the presence of HCl (compare Figs. 12 and 3). A noticeable difference in the reaction rates for TFA- and HCl-promoted oxidations is apparently the consequence of the higher coordination ability of chloride anion in comparison with trifluoroacetate. Thus, we can assume that Cl^- enters into the coordination sphere of the active copper species increasing its reactivity.

Using ESR spectroscopy, we studied the changes in the total copper(II) concentration ($[Cu^{II}]_{total}$) in the course of the interaction of **1** with TFA and H_2O_2. Concentration $[Cu^{II}]_{total}$ increases during 1 h of interaction of **1** with TFA approaching a constant value (Fig. 13, graph A). Addition of H_2O_2 at the beginning of the interaction leads to $[Cu^{II}]_{total}$ growth only after 10 min of the reaction (Fig. 13, graph B). H_2O_2 addition to the sample under conditions of Fig. 13, graph A, after 10 min of the reaction results in total disappearance of copper(II) complexes in the reaction mixture for about 20 min, then $[Cu^{II}]_{total}$ increases again (Fig. 13, graph C; Fig. 14). At higher concentration of Cu(II), the same system displays an ESR spectrum with resolved components at $g_{\parallel} = 2.37$, $g_{\perp} = 2.08$ (see Supporting Information, Fig. S7). These *g*-values are diagnostic of copper(II) complexes, either mononuclear or multinuclear with at least one non-interacting copper atom [65–67].

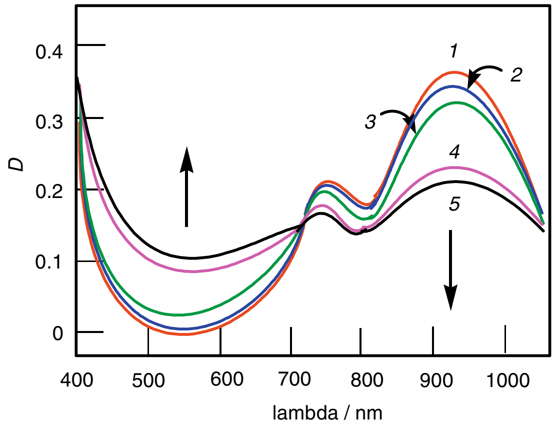

Fig. 12. Changes in the electronic spectrum of the solution in the course of the cyclohexane oxidation reaction. Conditions: 50 °C; solvent was acetonitrile (total volume of the reaction solution was 5 mL). Curves 1: a solution of **1** (1 mM) and cyclohexane (0.46 M); 2: TFA (4 mM) is added; 3: H_2O_2 (0.5 M) is added; 4: 20 min after the addition of H_2O_2; 5: 80 min after the addition of H_2O_2.

The dependence of W_0 on the concentration of catalyst **1** at variable and fixed concentrations of water exhibits a maximum at [1] ≈1 mM (Fig. 15). The maximum can be clearly seen also on the curve of the W_0–[TFA] dependence corresponding to the ratio [TFA]:[1] = 4 (Fig. 16), what indicates that only one proton is required to activate each copper triethanolaminate moiety of **1** and to reach the optimal performance in cyclohexane oxidation. Hence, it is reasonable to assume that **1** reacts through monoprotonation of each triethanolaminate ligand with cleavage of the corresponding $Cu–O(H)_{triethanolaminate}$ bond. Rupture of Cu–O bond can also occur upon protonation of the bridging oxo-ligand. Such cleavages should promote the reactivity due to the generated metal unsaturation.

As in the case of the reaction promoted by HCl, the addition of water also accelerates the oxidation in the system with TFA (Fig. 17). The important promoting role of water is also evident from Fig. 18, which shows the kinetic curves at two different concentrations of H_2O (i.e. 3.27 and 7.00 M), for constant concentrations of all the other reagents. It can be clearly seen that at higher $[H_2O]$ the induction period is short (ca. 10 min), while at lower $[H_2O]$ it is longer and ends after ca. 40 min reaction time. Similarly to the case of HCl, the dependence of W_0 on the initial concentration of cyclohexane has a plateau at $[CyH]_0 > 0.2$ M (Fig. 19). The dependence of W_0 on the initial concentration of hydrogen peroxide is linear in the interval $0 < [H_2O_2]_0 < 1$ M (Fig. 20). Although the TFA co-catalyst shows a noticeable promoting effect, it concedes to that of HCl, showing only the maximum W_0 and TOF values of ca. 25×10^{-6} M s^{-1} (Figs. 18 and 20) and 90 h^{-1} (Fig. S8), respectively.

4. Discussion

4.1. The nature of the oxidizing species

The mode of dependence of the cyclohexane, CyH, oxidation on its initial concentration in the presence of HCl (Fig. 9) and TFA (Fig. 19) is in accordance with the assumption that the oxidation is induced by an active oxidizing species X which is generated by the catalytic system. At a high concentration of CyH, the rate of its oxidation is maximal, it does not depend on $[CyH]_0$ and corresponds to the rate of generation of the oxidizing species. At a low concentration of CyH, the rate of the alkane oxidation is lower because not all the generated oxidizing species interact with CyH.

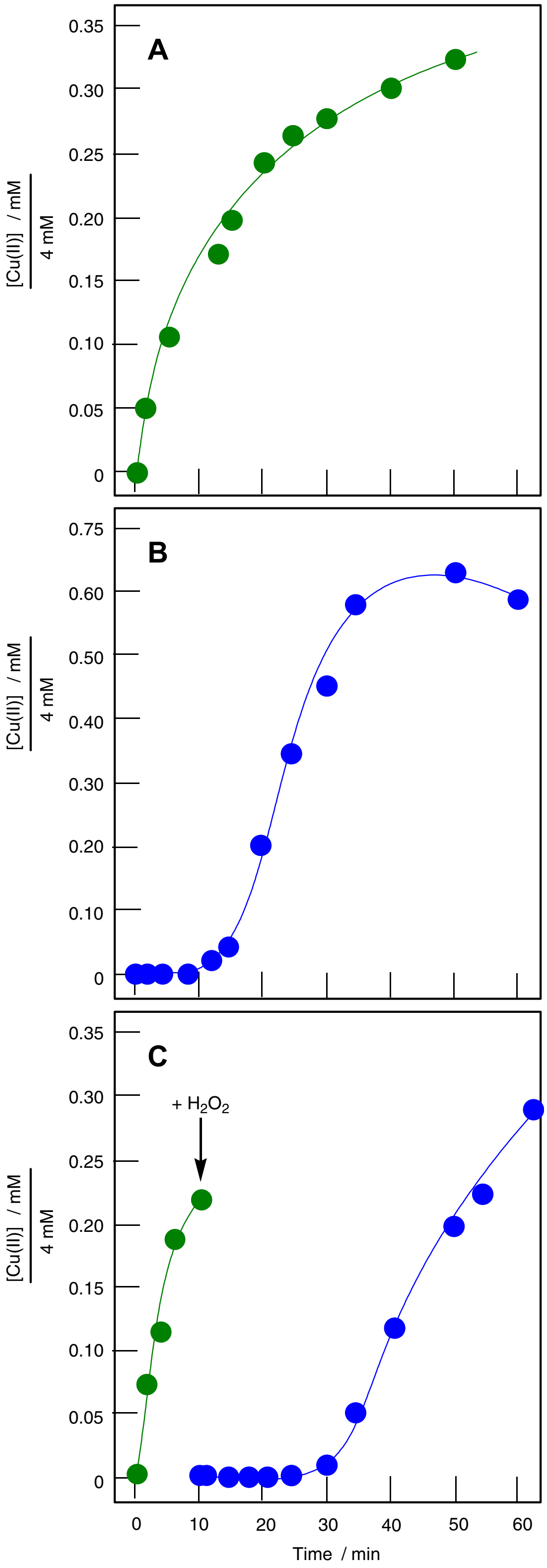

Fig. 13. Changes in the ESR spectra of the solutions of compound **1** (1 mM) in MeCN/H_2O (10:1 v/v) mixture after the addition (at time = 0) of TFA (4 mM). Graph A: hydrogen peroxide was not added. Graph B: H_2O_2 (0.5 M) was added simultaneously with TFA. Graph C: H_2O_2 (0.5 M) was added after 10 min (denoted with an arrow). The reaction was carried out at 50 °C, the ESR spectra were recorded at liquid nitrogen temperature. The [Cu(II)] (mM) /4 mM ratio (dimensionless value, where 4 mM is the total initial concentration of the four Cu^{II} of **1**) versus time is plotted. For the original ESR spectra used in graph C, see Fig. 14.

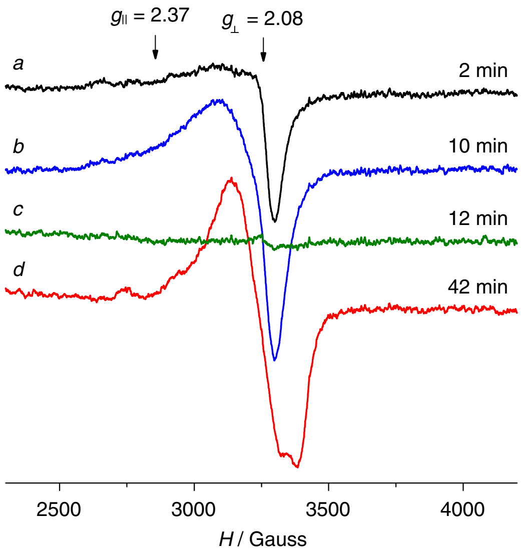

Fig. 14. The ESR spectra at different times used in Fig. 13, graph C.

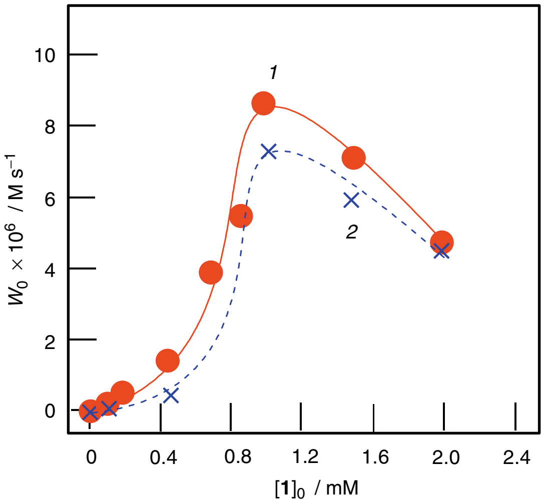

Fig. 15. Oxidation of cyclohexane (0.46 M) with hydrogen peroxide (50% aqueous; 0.5 M) catalyzed by compound **1** in the presence of TFA (4 mM) in MeCN at 50 °C. Dependences of the initial rate of oxygenate formation W_0 on initial concentration of catalyst **1** are shown. Curve 1: the oxidation at constant total concentration of water in all experiments (3.27 M); curve 2: the oxidation at varied concentration of water in the interval 1.16–3.27 M. Concentrations of cyclohexanone and cyclohexanol were determined after the reduction of the aliquots with solid PPh_3.

In the last case, the pathways of interaction between the transient active oxidizing species with other oxidizable components of the system become important and they compete with CyH in the oxidation process. Previously we assumed [63,68] that in other our systems with such a mode of dependence of W_0 on $[CyH]_0$ (Figs. 9 and 19), the solvent (acetonitrile) is the substance which plays the role of a substrate competing with CyH for the oxidizing species. Assuming that in the system under consideration acetonitrile also competes with cyclohexane for the oxidizing species X, we can create the following kinetic scheme.

$$H_2O_2 + \mathbf{1} \xrightarrow{(H^+, H_2O)} X \tag{i}$$

$$X + CyH \rightarrow \text{products} \tag{1}$$

$$X + MeCN \rightarrow \text{products} \tag{2}$$

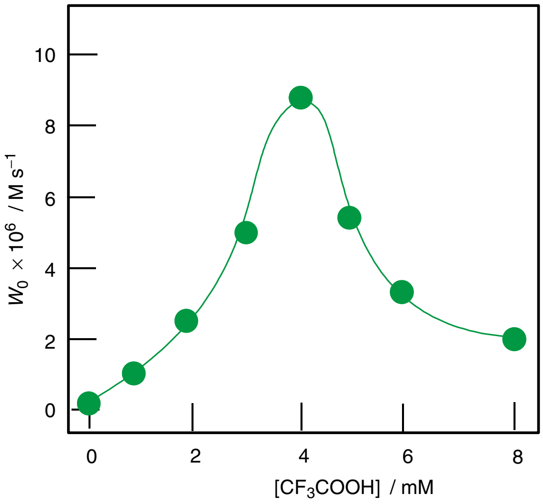

Fig. 16. Oxidation of cyclohexane (0.46 M) with hydrogen peroxide (50% aqueous; 0.5 M) catalyzed by compound **1** (1 mM) in the presence of TFA in MeCN at 50 °C. Dependence of the initial rate of oxygenate formation W_0 on concentration of added TFA is shown. Concentrations of cyclohexanone and cyclohexanol were determined after reduction of the aliquots with solid PPh_3.

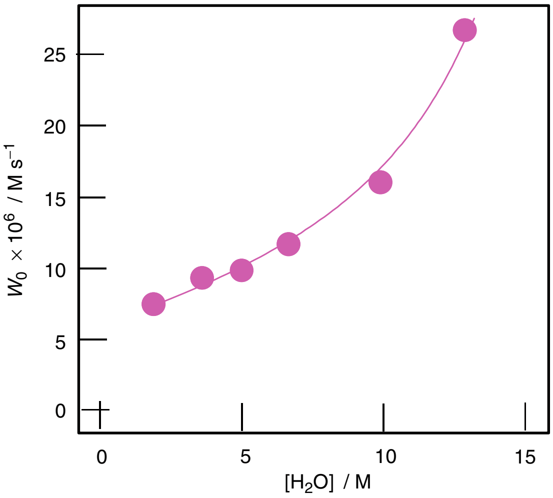

Fig. 17. Oxidation of cyclohexane (0.46 M) with hydrogen peroxide (50% aqueous; 0.5 M) catalyzed by compound **1** (1 mM) in the presence of TFA (4 mM) in MeCN at 50 °C. Dependence of the initial rate of oxygenate formation W_0 on total concentration of water present in the solution is shown. Concentrations of cyclohexanone and cyclohexanol were determined after the reduction of the aliquots with solid PPh_3.

Here (i) is the effective reaction of generation of the active species X by the catalytic system with the rate W_i. The main initial product formed from cyclohexane is cyclohexyl hydroperoxide. Acetonitrile is a relatively inert solvent that is successfully used in various oxidative transformations of alkanes [2,3,31]. However, it has been shown previously [69] that MeCN can be oxidized with the participation of hydroxyl radicals affording formaldehyde, formic acid and CO_2. Besides, peroxyimidic acid can be also generated from MeCN in a basic medium [70]. Nevertheless, under the mild slightly acidic conditions of the present work, the oxidation of acetonitrile is not appreciable. Indeed, we have found (see below) that the ratio between the rate constants of acetonitrile (k_2) and cyclohexane (k_1) oxidation is ca. 0.006. The analysis of the kinetic scheme (i), (1), (2) based on an assumption that the concentration of X is quasi-stationary led to Eq. (3) for the cyclohexane oxidation rate.

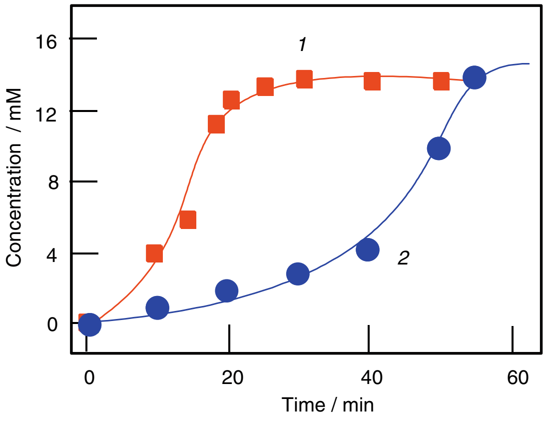

Fig. 18. Accumulation of oxygenates with time in cyclohexane (0.46 M) oxidation with hydrogen peroxide (50% aqueous; 0.5 M) catalyzed by compound **1** (1 mM) in the presence of TFA (4 mM) in MeCN at 50 °C at different contents of water. Curve 1: total content of water 7 M, curve 2: total content of water 3.27 M. Concentrations of cyclohexanone and cyclohexanol were determined after the reduction of the aliquots with solid PPh_3.

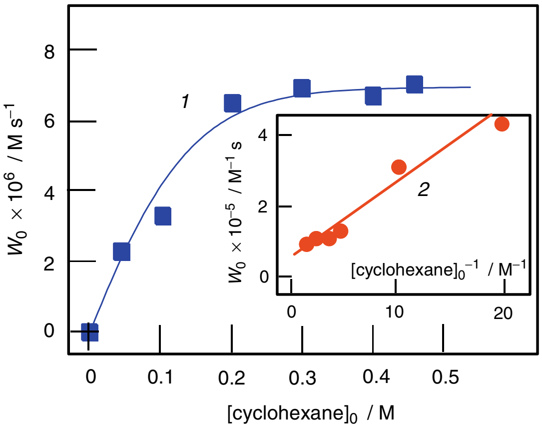

Fig. 19. Oxidation of cyclohexane with hydrogen peroxide (50% aqueous; 0.5 M; the total content of water in the reaction mixture was 1.17 M) catalyzed by compound **1** (1 mM) in the presence of TFA (4 mM) in MeCN at 50 °C. Dependence of the initial rate of oxygenate formation W_0 on initial concentration of cyclohexane is shown (curve 1). Linearization of curve 1 in coordinates $[\mathrm{cyclohexane}]_0^{-1}$–$W_0$ is presented by line 2. Concentrations of cyclohexanone and cyclohexanol were determined after the reduction of the aliquots with solid PPh_3.

$$W_0 = \frac{d[\mathrm{CyH}]}{dt} = \frac{W_\mathrm{i}}{1 + \frac{k_2[\mathrm{MeCN}]}{k_1[\mathrm{CyH}]}} \qquad (3)$$

The ratio of rate constants for the interaction of species X with MeCN and CyH (k_2/k_1) characterizes the reactivity of X. This parameter can be used in the identification of the transient species X. It should be noted that the kinetic characteristic k_2/k_1 of the species X experimentally measured in accord with Eq. (3) does not depend on the proposed mechanism of the catalytic reaction and therefore the objective parameter k_2/k_1 can be used as a measure of the species X reactivity. It has been shown previously [63] that for hydroxyl radicals generated in the photolysis of H_2O_2 the value of the k_2/k_1 ratio is 0.01. A similar k_2/k_1 value has also been obtained for other systems operating with the formation of hydroxyl radicals [63,71].

The experimental data presented in Fig. 9 for the co-catalysis by HCl allow us to approximately determine the parameter k_2/k_1. Concentration of cyclohexanol at which the oxidation rate W_0 is equal to ½ of the maximal rate is $[\mathrm{CyH}]_0 = 0.1$ M and $k_2[\mathrm{MeCN}]/$

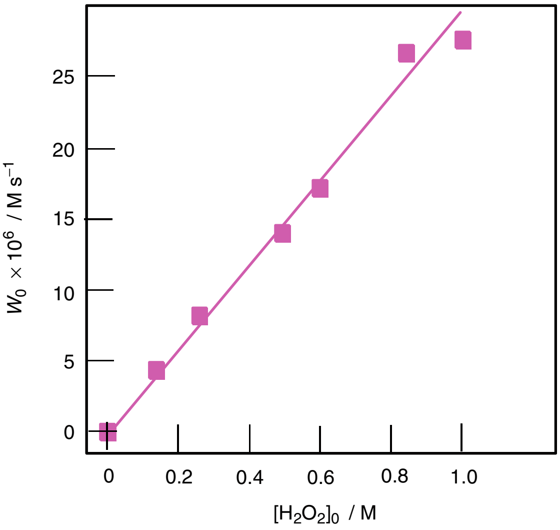

Fig. 20. Oxidation of cyclohexane with hydrogen peroxide (50% aqueous; the total content of water in the reaction mixture was constant = 7.0 M) catalyzed by compound **1** (1 mM) in the presence of TFA (4 mM) in MeCN at 50 °C. Dependence of the initial rate of oxygenate formation W_0 on initial concentration of H_2O_2 is shown. Concentrations of cyclohexanone and cyclohexanol were determined after the reduction of the aliquots with solid PPh_3.

$k_1[CyH] = 1$. As $[MeCN] \approx 17$ M, the value $k_2/k_1 \approx 0.006$ is obtained, being close to the value 0.01 measured in the photochemical generation of hydroxyl radicals. The dependence of W_0 on $[CyH]_0$ for the case of co-catalysis by TFA allows us to check if there is an agreement between the experimental data (Fig. 19, curve 1) and Eq. (3). It can be seen that the dependence of W_0^{-1} on $[CyH]_0^{-1}$ is depicted as a straight line (curve 2) which is in accord with Eq. (3). This fact supports the proposed kinetic model. In accordance with these data, the k_2/k_1 of 0.012 is estimated, being identical to that (0.01) [63,71] typical for the reaction mechanisms that proceed via the interaction of cyclohexane and acetonitrile with hydroxyl radicals. Thus, on the basis of kinetic data we can conclude that both catalytic systems under consideration (containing HCl and CF_3COOH) generate hydroxyl radicals as active oxidizing species. To get an additional support for this proposal, we measured the selectivity parameters in oxidations of certain linear, branched and cyclic saturated hydrocarbons. The results are summarized in Table 1, where the data for some other oxidizing systems are given for comparison. The regioselectivity parameters determined for the oxidation, by the systems under consideration (entries 1–3) and copper nitrate (entry 4), of *n*-heptane and *n*-octane are relatively low, i.e. C(1):C(2):C(3):C(4) ≈ 1:(5–10):(5–10):(5–10). These values are close to the parameters determined previously for systems which oxidize alkanes with the participation of hydroxyl radicals (compare with the parameters summarized in entries 5–9 of Table 1). The corresponding selectivity parameters for the systems that do not involve active oxygen-centred radicals (entries 9–12) are noticeably higher. As in the case of linear alkanes, the bond-selectivity parameter (1°:2°:3°) in the oxidation of methylcyclohexane catalyzed by **1** is close to the corresponding values found for the systems oxidizing alkanes with hydroxyl radicals (compare with the parameters summarized in entries 5–10). The oxidation of *cis*- and *trans*-1,2-dimethylcyclohexanes proceeds non-stereoselectively as the *trans/cis* ratios of isomeric alcohols (after reduction with PPh_3) were of ca. 1 (Table 1). The corresponding selectivity parameters for the systems that do not involve active oxygen-centred radicals (entries 11 and 12) can be noticeably higher. Thus, on the basis of the selectivity parameters, we can also assume that the alkane oxidation reactions catalyzed by compound **1** proceed via the formation of hydroxyl radicals.

4.2. Effect of added acids

Addition to the reaction mixture of the acids we have tested (HCl, H_2SO_4, HNO_3 and CF_3COOH) leads to a significant increase of the oxidation rates and changes the kinetic curves (Figs. 1 and 2). Although the role of such acid co-catalysts remains not fully established, one should mention their expected participation in proton-transfer steps leading to the activation of **1** via protonation of ligands (triethanolaminate and/or bridging oxo), and the promotion of unsaturation of the copper centres, as well as in the enhancement of the oxidizing properties of the metal and of hydrogen peroxide (the decomposition of the latter can also be suppressed in acidic medium) [31,33,36]. It should be noted that the effects of HNO_3 and CF_3COOH are similar and the reaction rate depends on the acid concentration (Fig. 16). For example, the reaction rate growths upon increasing the acid concentration from 0 to $[TFA] = 4[\mathbf{1}]_0$, presumably affording catalytically active species upon reductive transformations with the participation of H_2O_2 (see below). The decrease of the reaction rate at $[TFA] > 4[\mathbf{1}]_0$ is probably due to the decrease of the equilibrium concentration of H_2O_2 as a reducing reagent (HOO^-), as a result of shifting the equilibrium (4) to the left when the acid concentration grows.

$$H_2O_2 \leftrightarrows HOO^- + H^+ \tag{4}$$

Alternatively, the reaction rate drop can be associated with the decreasing concentrations of copper(II) peroxo complexes formed as shown by the simplified Eq. (5), in line with increasing acid concentration (hereinafter, in all equations involving copper species, triethanolaminate and μ_4-oxo-ligands of **1** are omitted for the sake of clarity).

$$Cu^{II} + H_2O_2 \leftrightarrows Cu^{II}OOH + H^+ \tag{5}$$

The promoting behaviours of other strong (H_2SO_4 and HCl) and weak (CH_3COOH) acids are not similar and depend on the acid nature. Thus, we can assume that the role of these acids consists not only in the protonation of ligands in the starting compound **1**, but also in the formation of an intermediate species with copper ions and sulfate, chloride or acetate anions. To this regard, the remarkable promoting effect of HCl can be associated with the recognized ability of chloride ions to stabilize the Cu(I) oxidation state through the generation of species with terminal or bridging chloride ligands [77].

4.3. Formation of catalytically active species

When a low concentration of TFA is used, it is possible to clearly see an auto-acceleration on the kinetic curves (Fig. 11, curves 1 and 2). This mode indicates that a catalytically active form of the copper catalyst is generated in the beginning of the process upon protonation of the starting compound **1**. ESR is indicative of the formation of a species with at least one non-interacting Cu(II) atom. A further step occurring during the auto-acceleration period is the reduction of the formed Cu(II) species by H_2O_2 to afford a Cu(I) species that is stabilized in the acetonitrile solution. The generation of the active species that oxidizes alkanes occurs in the oxidation–reduction cycle of copper ions by hydrogen peroxide. Kinetic studies and the selectivity parameters (see above) indicate that this active oxidizing species is the hydroxyl radical, which is formed in the Fenton-type reaction of one-electron oxidation of Cu(I) by hydrogen peroxide with the formation of hydroxyl radical and Cu(II) (see below).

4.4. Oxidase versus catalase activities

It is evident from Fig. 11 (curves 1 and 4) that under the used experimental conditions (given in figure caption) the cyclohexane oxidation catalyzed by **1** + TFA approaches a plateau after ca. 60 min. This can be associated either with full consumption of the hydrogen peroxide at this time or with achievement of a sort of kinetic equilibrium, but not with the deactivation of the catalyst. This conclusion is supported by the experiment depicted by curve 4, where the addition of a new portion of hydrogen peroxide (in the concentration equal to that in the beginning of the reaction) to the reaction mixture after completing the oxidation leads to the additional formation of the oxygenates in concentrations slightly inferior to that after the first run. Along with a possible decrease of catalyst activity, the slightly lower concentrations of oxygenates in those subsequent tests can be associated with the dilution of the reaction mixture due to the increased water content coming with the new portions of H_2O_2. The second and third runs occur without auto-acceleration which was typical for the first run. Moreover, the initial compound **1** can be easily recovered in a crystalline form from the reaction mixture at the end of reaction in an amount close to the initial one. This important feature indicates that the ligands at copper ions are not oxidized in the course of the reaction and the transformations of complex **1** are reversible, thus allowing its multiple recycling.

Taking into account that for $[CyH]_0 > 0.2$ M all active species generated by the system are accepted by the alkane and the solvent (Figs. 9 and 19), we can propose that only a few percent of H_2O_2 decompose via the mechanism with participation of hydroxyl radicals. This is in line with the recognized ability of copper complexes to catalyze H_2O_2 decomposition [78]. A dependence of the CyH oxidation rate on $[\mathbf{1}]_0$ is close to quadratic at low initial concentration of **1** in both systems with HCl (Fig. 6) and TFA (Fig. 15) co-catalysts. This fact is indicative of uncommon second-order (with respect to catalyst) reaction kinetics, revealing that two copper ions take part in the rate-limiting step of the catalytic generation of hydroxyl radicals. The decrease of the cyclohexane oxidation rate at higher concentration of **1** (>1 mM for the case of CF_3COOH) is apparently due to the decomposition of substantial amount of H_2O_2 via the catalase mechanism before attaining the maximum reaction rate. Indeed, the part of H_2O_2 which is involved into the CyH oxidation is decreased at high concentration of **1** while the part of hydrogen peroxide which decomposes via the catalase mechanism increases.

4.5. On the mechanism of the generation of hydroxyl radicals

On the basis of all obtained experimental data, the simplified catalytic reaction Scheme 2 can be proposed. In the first step *a*, the tetranuclear copper complex **1** is transformed, upon protonation by the acid co-catalyst, into a species $L\mathrm{Cu^{II}}$ that bears at least one non-interacting Cu(II) atom.

The ESR spectra demonstrate the accumulation of such a type of species with time (see Fig. 13, graph A). This transformation is rather fast when using HCl, while the lag period can be seen in the reaction promoted by TFA. Complex $L\mathrm{Cu^{II}}$ is not the active species towards the alkane because the preliminary incubation of the catalyst precursor **1** with trifluoroacetic acid does not remove the lag period (Fig. 11, curve 2).

In the subsequent step *b*, species $L\mathrm{Cu^{II}}$ reacts with H_2O_2 to produce a peroxo derivative $L\mathrm{Cu^{II}OOH}$ which, by reaction with the parent $L\mathrm{Cu^{II}}$ (step *c*) gives two reduced $L\mathrm{Cu^{I}}$ species with a dioxygen molecule and the proton. This step *c* is a rate-limiting process which is responsible for the second-order in respect to the catalyst precursor **1**. It can occur via a $L\mathrm{Cu^{II}OOH} + L\mathrm{Cu^{II}}$ combination with

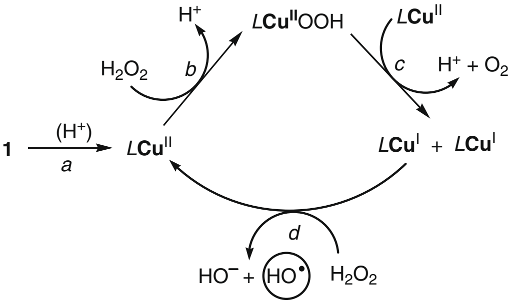

Scheme 2. A simplified catalytic cycle proposed for the formation of radicals in the $\mathbf{1}$–H^+–H_2O_2–H_2O/MeCN system.

transfer (reaction (6)) of two electrons from the hydrogen peroxide anion to the two copper(II) ions.

$$\overset{\curvearrowleft\, e^-}{L\mathrm{Cu^{II}}\quad \mathrm{HOO}} \overset{e^-\curvearrowright}{-\!\!-\,\mathrm{Cu^{II}}L} \longrightarrow 2\,L\mathrm{Cu^{I}} + \mathrm{H^+} + \mathrm{O_2} \tag{6}$$

The overall (*b* + *c*) reaction corresponds to the reduction of two $L\mathrm{Cu^{II}}$ molecules by one H_2O_2 molecule to afford two $L\mathrm{Cu^{I}}$ (reaction (7)). In accord with this, the ESR spectra show that the addition of H_2O_2 leads to the disappearance of $L\mathrm{Cu^{II}}$ due to its reduction to a Cu(I) derivative.

$$L\mathrm{Cu^{II}} + \mathrm{H_2O_2} + L\mathrm{Cu^{II}} \rightarrow 2L\mathrm{Cu^{I}} + 2\mathrm{H^+} + \mathrm{O_2} \tag{7}$$

Species $L\mathrm{Cu^{I}}$ is believed to be catalytically active, since the incubation of **1** with both TFA and H_2O_2 eliminates the lag period (see Fig. 11, curve 3). It reduces H_2O_2 to produce the hydroxyl radical with regeneration of $L\mathrm{Cu^{II}}$ (step *d*, Scheme 2; reaction (8)).

$$L\mathrm{Cu^{I}} + \mathrm{H_2O_2} \rightarrow L\mathrm{Cu^{II}} + \mathrm{HO^{\cdot}} + \mathrm{HO^-} \tag{8}$$

The interaction of copper-containing species with hydrogen peroxide proceeds apparently via the intermediate formation of unstable peroxo complexes. Various peroxo derivatives of copper [79] are well known to take part in biological [80–82] and chemical [83,84] oxidations with the participation of copper ions. It should be noted that dinuclear copper peroxo complexes [85–89] are the most common in such transformations, although tetracopper peroxo compounds are also known [90,91]. It has been recently shown that the addition of hydrogen peroxide to aqueous solutions of dicopper complexes produces an intermediate that subsequently decays with the concomitant generation of the hydroxyl radical [92]. Besides, light irradiation is known to enhance the ability of copper to undergo Fenton-like reactivity with the generation of hydroxyl radicals [93].

The hydroxyl radical generated in step *d* (see also reaction (8)) attacks the hydrocarbon molecule, RH, abstracting a hydrogen atom to produce the alkyl radical (reaction (9)) which rapidly reacts with molecular oxygen present in the solution to form the alkylperoxyl radical $ROO^{\cdot}$ (reaction (10)).

$$\mathrm{RH} + \mathrm{HO^{\cdot}} \rightarrow \mathrm{R^{\cdot}} + \mathrm{H_2O} \tag{9}$$

$$\mathrm{R^{\cdot}} + \mathrm{O_2} \rightarrow \mathrm{ROO^{\cdot}} \tag{10}$$

The alkylperoxyl radical can be reduced by a Cu(I) ion to the corresponding anion which is further transformed into the main primary alkyl hydroperoxide product (reactions (11) and (12)).

$$\mathrm{ROO^{\cdot}} + \mathrm{Cu^{I}} \rightarrow \mathrm{ROO^-} + \mathrm{Cu^{II}} \tag{11}$$

$$\mathrm{ROO^-} + \mathrm{H^+} \rightarrow \mathrm{ROOH} \tag{12}$$

The resulting alkyl hydroperoxide would undergo the copper-assisted homolytic decomposition to yield the alkoxyl $RO^{\cdot}$ and alkylperoxyl $ROO^{\cdot}$ radicals (reactions (13) and (14), respectively) [1,3,32,54,94].

$$ROOH + Cu^{I} \rightarrow RO^{\cdot} + Cu^{II} + HO^{-} \quad (13)$$

$$ROOH + Cu^{II} \rightarrow ROO^{\cdot} + Cu^{I} + H^{+} \quad (14)$$

The alkoxyl radicals would form the alcohol (ROH) by H-abstraction from the alkane (Reaction (15)), while the peroxyl radicals would dismutate (Reaction (16)) furnishing both the alcohol and the ketone ($R'{=}O$) [3,32,54].

$$RO^{\cdot} + RH \rightarrow ROH + R^{\cdot} \quad (15)$$

$$2ROO^{\cdot} \rightarrow ROH + R'{=}O + O_2 \quad (16)$$

Although to a lesser extent, an alternative metal-free pathway for the decomposition of ROOH can also take place resulting in the formation of ROH and $R'{=}O$ [95,96].

5. Conclusions

In the present work, we have further explored the recognized [30,31] application of the tetracopper(II) triethanolaminate complex **1** for the oxidation of alkanes with hydrogen peroxide under mild conditions, by reporting the kinetic, selectivity and mechanistic aspects of this transformation. Based on the combination of experimental kinetic, ESR and UV–vis studies, it has been found that a slight modification of the type of acid promoter (co-catalyst) can affect substantially the reaction rate. Hence, although HNO_3 and TFA act in a similar way, other strong acid additives such as H_2SO_4 and HCl exhibit rather different behaviours. An important feature of the system promoted by HCl consists in the remarkable fast oxidation of cyclohexane that is characterized by the very high values of initial reaction rate W_0 (up to ca. 135×10^{-6} M s^{-1}) and TOF (up to ca. 600 h^{-1}). This high activity enhancement is only observed in the **1** + HCl system, whereas the promoting effect of hydrochloric acid on other copper complexes [57] or simple copper salts is comparable to those of other strong acids.

The study also disclosed an unusual promoting role of water showing that the rate of cyclohexane oxidation in acetonitrile is strongly dependent on the H_2O amount, following an increasing trend at higher concentrations of water (e.g. $W_0 = 15 \times 10^{-6}$ at 1 M H_2O versus $W_0 = 110 \times 10^{-6}$ M s^{-1} at 4 M H_2O; see Fig. 8). This contrasts significantly with the majority of state-of-the-art systems for alkane oxidations where water plays typically an inhibiting role. Such a promoting feature of H_2O can be also of potential practical importance, allowing the use of diluted aqueous solutions of hydrogen peroxide that are generated in situ. Although not yet fully established, the role of water in the present work conceivably consists on the solubilization and activation of catalyst, formation and stabilization of intermediate aqua- and/or hydroxo Cu complexes, as well as in the facilitation of H-transfer steps, crucial in the generation of $HO^{\cdot}$ radicals. To this regard, it should be mentioned that a "water-assisted" mechanism has been theoretically proposed in the $[MeReO_3]/H_2O_2/H_2O{-}CH_3CN$ system [60]. Furthermore, an unprecedented hydroxylating role of water has been recently disclosed by some of us and supported by radical trap, $H_2{}^{18}O$ and DFT studies in the aqueous-medium carboxylation of alkanes to carboxylic acids promoted by compound **1** [52].

Another interesting feature of the present work consists in the uncommon second-order concerning the catalyst reaction kinetics. This indicates that in the rate-limiting step two copper species react with one H_2O_2 molecule to generate hydroxyl radicals which attack the hydrocarbon. Besides, the kinetic and ESR investigations pointed out the catalyst precursor nature of **1** which, under the action of an acid, hydrogen peroxide and water, is transformed into catalytically active Cu(I) species. The latter was found to not be deactivated in the course of alkane oxidation, allowing its multiple recycling.

The observed features of the **1** + HCl catalytic system should be taken into consideration in future developments towards exploring the mild oxidative transformations of other alkanes and employing cheaper oxidants (air or dioxygen) rather than hydrogen peroxide. Given the high activity and recyclability of **1**, further work is currently in progress aiming at its heterogenization on various supports and the establishment of the catalytic potential for alkane oxidations under heterogeneous conditions.

Acknowledgments

The authors thank the Foundation for Science and Technology (FCT), its PPCDT and "Science 2007" programs (FEDER funded), and the Russian Foundation for Basic Research (Grant 06-03-32344-a) for support. L.S.S. and G.B.S. express their gratitude to the FCT for making it possible for them to stay at the Instituto Superior Técnico, TU Lisbon, as invited scientists and to perform a part of the present work.

Appendix A. Supplementary material

Supplementary data associated with this article can be found, in the online version, at doi:10.1016/j.jcat.2009.08.016.

References

[1] G. Strukul (Ed.), Catalytic Oxidations with Hydrogen Peroxide as Oxidant, Kluwer Academic Publishers, Dordrecht, The Netherlands, 1992.
[2] A.E. Shilov, G.B. Shul'pin, Chem. Rev. 97 (1997) 2879–2932.
[3] A.E. Shilov, G.B. Shul'pin, Activation and Catalytic Reactions of Saturated Hydrocarbons in the Presence of Metal Complexes, Kluwer, Boston, 2000.
[4] G.B. Shul'pin, Oxidations of C–H compounds catalyzed by metal complexes, in: M. Beller, C. Bolm (Eds.), Transition Metals for Organic Synthesis, Second ed., vol. 2, Wiley–VCH, Weinheim/New York, 2004, pp. 215–242.
[5] J.A. Labinger, J.E. Bercaw, Nature 417 (2002) 507–514.
[6] A.A. Fokin, P.R. Schreiner, Chem. Rev. 102 (2002) 1551–1593.
[7] A. Sen, Acc. Chem. Res. 31 (1998) 550–557.
[8] R.H. Crabtree, J. Organomet. Chem. 689 (2004) 4083–4091.
[9] R.A. Periana, O. Mironov, D. Taube, G. Bhalla, C.J. Jones, Science 301 (2003) 814–818.
[10] M. Zerella, S. Mukhopadhyay, A.T. Bell, Chem. Commun. (2004) 1948–1949.
[11] C. Jia, T. Kitamura, Y. Fujiwara, Acc. Chem. Res. 34 (2001) 633–639.
[12] T. Punniyamurthy, L. Rout, Coord. Chem. Rev. 252 (2008) 134–154.
[13] M.M. Días-Requejo, P.J. Pérez, Chem. Rev. 108 (2008) 3379–3394.
[14] T. Okuno, S. Ohba, Y. Nishida, Polyhedron 16 (1997) 3765–3774.
[15] S. Velusamy, T. Punniyamurthy, Tetrahedron Lett. 44 (2003) 8955–8957.
[16] G.B. Shul'pin, J. Gradinaru, Y.N. Kozlov, Org. Biomol. Chem. 1 (2003) 3611–3617.
[17] C. Bolm, J.-C. Frison, J. Le Paih, C. Moessner, Tetrahedron Lett. 45 (2004) 5019–5021.
[18] K. Shimizu, Y. Murata, A. Satsuma, J. Phys. Chem. C 111 (2007) 19043–19051.
[19] M.C. Esmelindro, E.G. Oestreicher, M. Caovilla, J.A. Lessa, C. Fernandes, C. Dariva, S.M. Egues, A.J. Bortoluzzi, O.A.C. Antunes, J. Braz. Chem. Soc. 17 (2006) 1551–1557.
[20] M.M. Maurya, M. Kumar, U. Kumar, J. Mol. Catal. A: Chem. 273 (2007) 133–143.
[21] M. Zhu, X. Wei, B. Li, Y. Yuan, Tetrahedron Lett. 48 (2007) 9108–9111.
[22] J. Pan, C. Wang, S. Guo, J. Li, Z. Yang, Catal. Commun. 9 (2008) 176–181.
[23] F.P. Canhota, G.C. Salomão, N.M.F. Carvalho, O.A.C. Antunes, Catal. Commun. 9 (2008) 182–185.
[24] Q. Tan, M. Hayashi, Adv. Synth. Catal. 350 (2008) 2639–2644.
[25] T.A. Balandina, T.Y. Larina, N.I. Kuznetsova, B.S. Bal'zhinimaev, Kinet. Catal. 49 (2008) 499–505.
[26] P. Roy, K. Dhara, M. Manassero, P. Banerjee, Eur. J. Inorg. Chem. (2008) 4404–4412.
[27] L.S. Shul'pina, K. Takaki, T.V. Strelkova, G.B. Shul'pin, Petrol. Chem. 48 (2008) 219–222.
[28] P. Chutia, S. Kato, T. Kojima, S. Satokawa, Polyhedron 28 (2009) 370–380.
[29] Y. Du, Y. Xiong, J. Li, X. Yang, J. Mol. Catal. A: Chem. 298 (2009) 12–16.
[30] A.M. Kirillov, M.N. Kopylovich, M.V. Kirillova, M. Haukka, M.F.C.G. da Silva, A.J.L. Pombeiro, Angew. Chem., Int. Ed. 44 (2005) 4345–4349.
[31] A.M. Kirillov, M.N. Kopylovich, M.V. Kirillova, E.Y. Karabach, M. Haukka, M.F.C.G. da Silva, A.J.L. Pombeiro, Adv. Synth. Catal. 348 (2006) 159–174.

[32] Y.Y. Karabach, A.M. Kirillov, M. Haukka, M.N. Kopylovich, A.J.L. Pombeiro, J. Inorg. Biochem. 102 (2008) 1190–1194.
[33] D.S. Nesterov, V.N. Kokozay, V.V. Dyakonenko, O.V. Shishkin, J. Jezierska, A. Ozarowski, A.M. Kirillov, M.N. Kopylovich, A.J.L. Pombeiro, Chem. Commun. (2006) 4605–4607.
[34] C. Di Nicola, Y.Y. Karabach, A.M. Kirillov, M. Monari, L. Pandolfo, C. Pettinari, A.J.L. Pombeiro, Inorg. Chem. 46 (2007) 221–230.
[35] M.V. Kirillova, A.M. Kirillov, M.F.C.G. da Silva, A.J.L. Pombeiro, Eur. J. Inorg. Chem. (2008) 3423–3427.
[36] K.R. Gruenwald, A.M. Kirillov, M. Haukka, J. Sanchiz, A.J.L. Pombeiro, Dalton Trans. (2009) 2109–2120.
[37] G.V. Nizova, M.M. Kats, G.B. Shul'pin, Bull. Acad. Sci. USSR, Div. Chem. Sci. 39 (1990) 618–619.
[38] G.B. Shul'pin, G.V. Nizova, M.M. Kats, J. Gen. Chem. USSR 60 (1990) 2447–2449.
[39] P. Lederer, G.V. Nizova, M.M. Kats, G.B. Shul'pin, Coll. Czech. Chem. Commun. 57 (1992) 107–112.
[40] G.B. Shul'pin, G.V. Nizova, Petrol. Chem. 33 (1993) 107–112.
[41] G.B. Shul'pin, M.M. Bochkova, G.V. Nizova, J. Chem. Soc. Perkin Trans. 2 (1995) 1465–1469.
[42] K. Takaki, J. Yamamoto, Y. Matsushita, H. Morii, T. Shishido, K. Takehira, Bull. Chem. Soc. Jpn. 76 (2003) 393–398.
[43] K. Takaki, Y. Yamamoto, K. Komeyama, T. Kawabata, K. Takehira, Bull. Chem. Soc. Jpn. 77 (2004) 2251–2255.
[44] R. Galiasso Tailleur, C.J.G. García, J. Catal. 250 (2007) 110–120.
[45] Y. Li, M. Wu, W. Liu, Z. Yi, J. Zhang, Catal. Lett. 123 (2008) 123–128.
[46] G. Izzet, J. Zeitouny, H. Akdas-Killig, Y. Frapart, S. Ménage, B. Douziech, I. Jabin, Y. Le Mest, O. Reinaud, J. Am. Chem. Soc. 130 (2008) 9514–9523.
[47] S.I. Chan, V.C.-C. Wang, J.C.-H. Lai, S.S.-F. Yu, P.P.-Y. Chen, K.H.-C. Chen, C. -Li Chen, M.K. Chan, Angew. Chem., Int. Ed. 46 (2007) 1992–1994.
[48] R.L. Lieberman, A.C. Rosenzweig, Nature 434 (2005) 177–182.
[49] Y.Y. Karabach, A.M. Kirillov, M. Haukka, J. Sanchiz, M.N. Kopylovich, A.J.L. Pombeiro, Cryst. Growth Des. 8 (2008) 4100–4108.
[50] A.M. Kirillov, Y.Y. Karabach, M. Haukka, M.F.C. Guedes da Silva, J. Sanchiz, M.N. Kopylovich, A.J.L. Pombeiro, Inorg. Chem. 47 (2008) 162–175.
[51] Y.Y. Karabach, A.M. Kirillov, M.F.C.G. da Silva, M.N. Kopylovich, A.J.L. Pombeiro, Cryst. Growth Des. 6 (2006) 2200–2203.
[52] M.V. Kirillova, A.M. Kirillov, M.L. Kuznetsov, J.A.L. Silva, J.J.R. Fraústo da Silva, A.J.L. Pombeiro, Chem. Commun. (2009) 2353–2355.
[53] P.J. Figiel, A.M. Kirillov, Y.Y. Karabach, M.N. Kopylovich, A.J.L. Pombeiro, J. Mol. Catal. A: Chem. 305 (2009) 178–182.
[54] G.B. Shul'pin, J. Mol. Catal. A: Chem. 189 (2002) 39–66.
[55] G.B. Shul'pin, CR Chimie 6 (2003) 163–178.
[56] G.B. Shul'pin, Mini-Rev. Org. Chem. 6 (2009) 95–104.
[57] U. Schuchardt, D. Cardoso, R. Sercheli, R. Pereira, R.S. da Cruz, M.C. Guerreiro, D. Mandelli, E.V. Spinace, E.L. Pires, Appl. Catal. A 211 (2001) 1.
[58] Ullmann's Encyclopedia of Industrial Chemistry, 6th ed., Wiley-VCH, Weinheim, 2002.
[59] M.G. Gichinga, S. Striegler, J. Am. Chem. Soc. 130 (2008) 5150–5156.
[60] M.L. Kuznetsov, A.J.L. Pombeiro, Inorg. Chem. 48 (2009) 307–318.
[61] G.B. Shul'pin, Y.N. Kozlov, G.V. Nizova, G. Süss-Fink, S. Stanislas, A. Kitaygorodskiy, V.S. Kulikova, J. Chem. Soc. Perkin Trans. 2 (2001) 1351–1371.
[62] Y.N. Kozlov, V.B. Romakh, A. Kitaygorodskiy, P. Buglyó, G. Süss-Fink, G.B. Shul'pin, J. Phys. Chem. A 111 (2007) 7736–7752.
[63] G.B. Shul'pin, G.V. Nizova, Y.N. Kozlov, L. Gonzalez Cuervo, G. Süss-Fink, Adv. Synth. Catal. 346 (2004) 317–332.
[64] G.B. Shul'pin, G. Süss-Fink, L.S. Shul'pina, J. Mol. Catal. A: Chem. 170 (2001) 17–34.
[65] H.R. Gersmann, J.D. Swalen, J. Chem. Phys. 36 (1962) 3221–3233.
[66] S.J.T. Owen, K.J. Standley, A. Walker, J. Chem. Phys. 40 (1964) 183–186.
[67] E.M. Roberts, W.S. Koski, J. Am. Chem. Soc. 83 (1961) 1865–1867.
[68] Y.N. Kozlov, G.V. Nizova, G.B. Shul'pin, J. Mol. Catal. A: Chem. 227 (2005) 247–253.
[69] G. Süss-Fink, G.V. Nizova, S. Stanislas, G.B. Shul'pin, J. Mol. Catal. A: Chem. 130 (1998) 163–170.
[70] G.B. Shul'pin, M.V. Kirillova, T. Sooknoi, A.J.L. Pombeiro, Catal. Lett. 123 (2008) 135–141.
[71] D. Mandelli, K.C. Chiacchio, Y.N. Kozlov, G.B. Shul'pin, Tetrahedron Lett. 49 (2008) 6693–6697.
[72] L.S. Shul'pina, M.V. Kirillova, A.J.L. Pombeiro, G.B. Shul'pin, Tetrahedron 65 (2009) 2424–2429.
[73] G.B. Shul'pin, J. Chem. Res. (S) (2002) 351–353.
[74] G.B. Shul'pin, A.R. Kudinov, L.S. Shul'pina, E.A. Petrovskaya, J. Organomet. Chem. 691 (2006) 837–845.
[75] G.B. Shul'pin, G. Süss-Fink, A.E. Shilov, Tetrahedron Lett. 42 (2001) 7253–7256.
[76] G.B. Shul'pin, M.G. Matthes, V.B. Romakh, M.I.F. Barbosa, J.L.T. Aoyagi, D. Mandelli, Tetrahedron 64 (2008) 2143–2152.
[77] See the Cambridge Structural Database (CSD, version 5.30, February 2009): F.H. Allen, Acta Cryst. B58 (2002) 380–388.
[78] I. Schepetkin, A. Potapov, A. Khlebnikov, E. Korotkova, A. Lukina, G. Malovichko, L. Kirpotina, M.T. Quinn, J. Biol. Inorg. Chem. 11 (2006) 499–513.
[79] S. Yamaguchi, S. Nagatomo, T. Kitagawa, Y. Funahashi, T. Ozawa, K. Jitsukawa, H. Masuda, Inorg. Chem. 42 (2003) 6968–6970.
[80] A. Rozenzweig, M.H. Sazinsky, Curr. Opin. Struct. Biol. 16 (2006) 729–735.
[81] A. De, S. Mandal, R. Mukherjee, J. Inorg. Biochem. 102 (2008) 1170–1189.
[82] R.A. Himes, K.D. Karlin, Curr. Opin. Chem. Biol. 13 (2009) 119–131.
[83] T. Matsumoto, H. Furutachi, M. Kobino, M. Tomii, S. Nagatomo, T. Tosha, T. Osako, S. Fujinami, S. Itoh, T. Kitagawa, M. Suzuki, J. Am. Chem. Soc. 128 (2006) 3874–3875.
[84] Y. Lee, D.-H. Lee, A.A.N. Sarjeant, L.N. Zakharov, A.L. Rheingold, K.D. Karlin, Inorg. Chem. 45 (2006) 10098–10107.
[85] Y. Tachi, K. Aita, S. Termae, F. Tani, Y. Naruta, S. Fukuzumi, S. Itoh, Inorg. Chem. 43 (2004) 4558–4560.
[86] L.Q. Hatcher, D.-H. Lee, M.A. Vance, A.E. Milligan, R. Sarangi, K.O. Hodgson, B. Hedman, E.I. Solomon, K.D. Karlin, Inorg. Chem. 45 (2006) 10055–10057.
[87] T. Matsumoto, H. Furutachi, S. Nagatomo, T. Tosha, S. Fujinami, T. Kitagawa, M. Suzuki, J. Organomet. Chem. 692 (2007) 111–121.
[88] D. Maiti, H.C. Fry, J.S. Woertink, M.A. Vance, E.I. Solomon, K.D. Karlin, J. Am. Chem. Soc. 129 (2007) 264–265.
[89] H.R. Lucas, L. Li, A.A.N. Sarjeant, M.A. Vance, E.I. Solomon, K.D. Karlin, J. Am. Chem. Soc. 131 (2009) 3230–3245.
[90] F. Meyer, H. Pritzkow, Angew. Chem., Int. Ed. 39 (2000) 2112–2115.
[91] J. Reim, R. Werner, W. Haase, B. Krebs, Chem. Eur. J. 4 (1998) 289–298.
[92] Q. Zhu, Y. Lian, S. Thyagarajan, S.E. Rokita, K.D. Karlin, N.V. Blough, J. Am. Chem. Soc. 130 (2008) 6304–6305.
[93] K.L. Ciesienski, K.L. Haas, M.G. Dickens, Y.T. Tesema, K.J. Franz, J. Am. Chem. Soc. 130 (2008) 12246–12247.
[94] M.V. Kirillova, A.M. Kirillov, P.M. Reis, J.A.L. Silva, J.J.R. Fraústo da Silva, A.J.L. Pombeiro, J. Catal. 248 (2007) 130–136.
[95] L.V. Petrov, T.I. Drozdova, L.Y. Lyuta, V.M. Solyanikov, Russ. Chem. Bull. 39 (1990) 226–232.
[96] I. Toth, Patent WO/2006/066904, 2006.